Third-Order Nonlinear Optical Response near the Plasmon Resonance Band of $Cu_{2-x}Se$ Nanocrystals *

Lan-Qing Zhou(周兰青)[1,2], Yan-Bang Zhang(张延榜)[3], Teng-Fei Yan(闫腾飞)[2], Ying Li(李莹)[2], Guo-Zhi Jia(贾国治)[3], Huai-Zhe Xu(许怀哲)[1], Xin-Hui Zhang(张新惠)[2,4]**

[1]*State Key Laboratory of Software Development Environment and Department of Physics, Beihang University, Beijing 100191*

[2]*State Key Laboratory of Superlattices and Microstructures, Institute of Semiconductors, Chinese Academy of Science, P. O. Box 912, Beijing 100083*

[3]*School of Science, Tianjin Chengjian University, Tianjin 300384*

[4]*College of Materials Science and Opto-electronic Technology, University of Chinese Academy of Sciences, Beijing 100049*

(Received 8 October 2016)

The third-order nonlinear optical properties of water-soluble $Cu_{2-x}Se$ nanocrystals are studied in the near infrared range of 700–980 nm using a femtosecond pulsed laser by the Z-scan technique. It is observed that the nonlinear optical response of $Cu_{2-x}Se$ nanocrystals is sensitively dependent on the excitation wavelength and exhibits the enhanced nonlinearity compared with other selenides such as ZnSe and CdSe. The W-shaped Z-scan trace, a mixture of the reversed saturated absorption and saturated absorption, is observed near the plasmon resonance band of $Cu_{2-x}Se$ nanocrystals, which is attributed to the state-filling of free carriers generated by copper vacancies (self-doping effect) of $Cu_{2-x}Se$ nanocrystals as well as the hot carrier thermal effect upon intense femtosecond laser excitation. The large nonlinear optical response and tunable plasmonic band make $Cu_{2-x}Se$ nanocrystals promising materials for applications in ultra-fast all-optical switching devices as well as nonlinear nanosensors.

PACS: 42.65.An, 42.70.Nq, 78.20.Ci DOI: 10.1088/0256-307X/34/1/014205

Semiconductor nanostructures of transition metal chalcogenides are known to exhibit a variety of fascinating properties and show promising applications as building blocks in electronics, optoelectronics, sensors, bio-imaging, and so on.[1,2] Moreover, semiconductor nanostructures of transition metal chalcogenides have also exhibited attractive nonlinear optical properties such as nonlinear absorption,[3] nonlinear refraction[4] and optical limiting,[5,6] benefiting from the strong confinement of excitons. More importantly, extensive research efforts have been devoted recently to the coupled hybrid nanostructures of semiconductor nanomaterials with noble metal nanocrystals such as Ag and Au,[7–13] which have been demonstrated to possess unique linear and nonlinear optical properties compared with their individual counterparts.[8,9,11,14–21]

Recently, the heavily-doped semiconductor nanocrystals of copper chalcogenides such as $Cu_{2-x}S$ and $Cu_{2-x}Se$ have emerged to draw great attention since they exhibit metallic behavior due to 'self-doping' by the existence of a large number of copper vacancies, and eventually a tunable plasmonic response in the near infrared (IR) wavelength range which is not easily accessed by noble metal nanocrystals.[22–29] In 2011, Dorfs *et al.* reported detailed studies of self-doping on the plasmonic properties of $Cu_{2-x}Se$ nanocrystals,[30] after successful preparation and plasmonic property studies of $Cu_{2-x}S$.[31,32] The silica sol-gel glasses embedded with copper selenides have also revealed both semiconductor-like absorption band and especially the near-IR absorption of plasmon resonance band which is associated with the band structure of $Cu_{2-x}Se$.[33–36] To the best of our knowledge, the third-order nonlinear optical response of copper selenide has been rarely studied so far, though a series of selenides such as ZnSe, CdSe, PbSe have been investigated extensively to show many interesting nonlinear optical properties.[3–6,37–39]

In this Letter, we report on a detailed experimental investigation of the nonlinear response of $Cu_{2-x}Se$ nanocrystals under femtosecond laser excitation in the near-infrared regime (700–980 nm), by performing the Z-scan technique. The maximum values of the nonlinear absorption coefficient and nonlinear refractive index are estimated to be 7.38×10^{-9} m/W and 2.64×10^{-15} m^2/W, respectively. The free carriers generated by copper vacancy (self-doping effect) of $Cu_{2-x}Se$ nanocrystals as well as the hot carrier thermal effect upon intense femtosecond laser excitation has been discussed to attribute to the enhanced third-order nonlinear response of $Cu_{2-x}Se$ nanocrystals near its plasmon resonance band.

The nanocrystals can be synthesized using the simple and rapid assisted-microwave method.[40,41] Here the powder $Cu_{2-x}Se$ nanocrystals are prepared based on the assisted-microwave method as follows: 0.397 g $CuCl_2{\cdot}2H_2O$, 0.201 g Na_2SeO_3, 0.467 g polyvinylpyrrolidone (PVP) and 0.249 g NaOH were placed into a three-necked flask, and ethylene glycol (EG) of 60 ml was added. The mixed solution was magnetically stirred at room temperature to obtain the homogeneous solution. Then the three-necked flask was transfer-

*Supported by the National Natural Science Foundation of China under Grant Nos 11274302, 11474276 and 11674240.

**Corresponding author. Email: xinhuiz@semi.ac.cn

© 2017 Chinese Physical Society and IOP Publishing Ltd

red into the microwave system (300 W) and heated at 180℃ for 1 h. To remove the excess PVP and ions, the products were centrifuged and washed with deionized water and ethanol three times, respectively. The as-prepared products were then dried at room temperature for further characterization. Figure 1(a) shows the powder x-ray diffraction (XRD) patterns of the $Cu_{2-x}Se$ nanocrystals, in which the main phase of $Cu_{2-x}Se$ nanocrystals is seen to be established (JCPDS 06-0680) and determined to be tetragonal. Due to the exposure of $Cu_{2-x}Se$ nanocrystals to air, the three main peaks of (111), (220) and (311) slightly shift to higher 2θ angles, indicating a decrease in the lattice parameters.[42] The peaks appearing at higher 2θ angles (>60°) are associated with the nonstoichiometric copper-deficient $Cu_{2-x}Se$.[42] The two peaks marked with asterisks in Fig. 1(a) are associated with Se residue in the as-prepared powder. The shapes of the synthesized $Cu_{2-x}Se$ nanocrystals are revealed to be hollow spheres as shown in the transmission electron microscopy (TEM) micrograph of Fig. 1(b), from which the averaged diameters of $Cu_{2-x}Se$ hollow spherical nanocrystals are ∼200 nm, with the shell thickness of ∼5 nm.

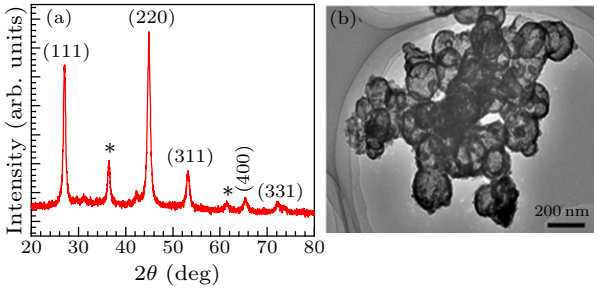

Fig. 1. (a) The powder x-ray diffraction pattern of the $Cu_{2-x}Se$ nanocrystals in which the two peaks marked with asterisks are associated with Se residue in the as-prepared powder. (b) TEM micrograph of $Cu_{2-x}Se$ nanocrystals.

The prepared powder is then dispersed in the deionized water assisted by the ultrasonic wave-stirring. Figure 2 shows the room temperature UV-VIS-NIR absorbance spectra of $Cu_{2-x}Se$ nanocrystals dispersed in water, which is characterized with a bandgap-related, monotonically rising absorbance at wavelength below 800 nm and a broad absorbance peak centered at ∼1050 nm associated with the plasmonic feature of $Cu_{2-x}Se$ nanocrystals, indicating that the composition of copper is about $x = 0.15$ for our studied $Cu_{2-x}Se$ nanocrystals, based on the calculated extinction spectrum of $Cu_{2-x}Se$ nanocrystals for different x by Dorfs *et al.*[30,42–44] The band gap E_g of $Cu_{2-x}Se$ nanocrystals can be evaluated by the absorbance spectra based on the relation of $\alpha_0 = A\sqrt{h\upsilon - E_g}$ (α_0 is the absorption coefficient), as shown in the inset of Fig. 2, giving the bandgap energy of ∼2.16 eV (571 nm). The water-dispersed sample is then injected into a 1-mm-thick quartz cuvette, which is mounted on a remotely controlled translation stage, thus it can move along the Z-axis. The Z-scan measurement is taken with a Ti:sapphire laser system (Chameleon Ultra Ⅱ, Coherent Inc.) which provides 150 fs pulse with repetition rate of 80 MHz. The excitation laser beam is focused onto the sample using a lens with a focal length of $f = 100$ mm and passes through a variable-diameter aperture which is placed before a silicon photodiode. Attenuators are used to control the intensity below the damage threshold. All the Z-scan results are normalized to the low-intensity-excitation case to avoid the perturbation signal caused by light scattering. The nonlinear absorption coefficient can be extracted from the open-aperture measurements and the sign and magnitude of the nonlinear refractive index can be determined by the closed-aperture Z-scan measurements.[45–48]

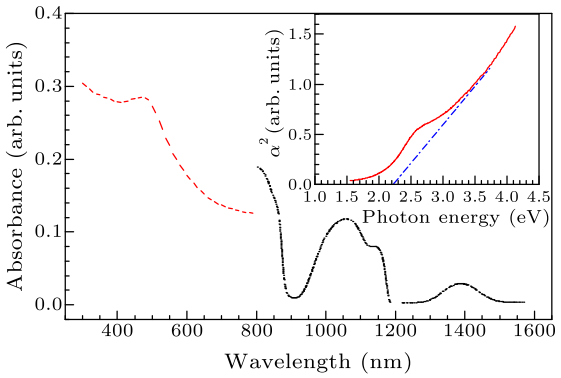

Fig. 2. Absorption spectrum of $Cu_{2-x}Se$ nanocrystals taken in the visible (red dashed line) and near infrared (black solid line) ranges, respectively. The direct bandgap is extracted to be ∼2.16 eV.

To elucidate the nonlinear absorption behavior of $Cu_{2-x}Se$ nanocrystals, open-aperture Z-scan measurements have been first carried out in the wavelength range of 700–980 nm at the same excitation intensity of 0.25 GW/cm^2, as displayed in Fig. 3. It is seen that the nonlinear absorption of $Cu_{2-x}Se$ nanocrystals exhibits quite complex behavior: it undergoes a transformation from a valley-shaped two-photon absorption in the range of 700–900 nm, and then a W-shaped complex feature above 950 nm when the excitation photon energy approaches to the near resonance of plasmon band of $Cu_{2-x}Se$ nanocrystals as seen in Fig. 2. It is known that the nonlinear absorption is contributed from different mechanisms such as two-photon absorption, free carrier absorption and the excited state absorption, depending on the excitation photon energy (wavelength) and pulse width.[39,46] These different mechanisms can often involve and compete with each other in the single Z-scan measurement, especially when the excitation photon energy is near the resonant band. The competing saturation absorption and free carrier absorption can lead to the observed W-shaped open-aperture Z-scan trace, which is a mixture of the reversed saturated absorption and saturated absorption, as the broad absorption band centered around 1050 nm is actually the plasmon resonant band of $Cu_{2-x}Se$ nanocrystals as previously reported.[30,42–44] Photoexcitation at plasmon reso-

nance band can induce a state-filling absorption bleaching effect caused by higher-order optical transition oscillators, due to the self-doping effect in $Cu_{2-x}Se$ nanocrystals. When the plasmon resonance band becomes excited, the excited hot carriers have different energies from that of the unexcited carrier. This causes a dynamic transition energy shift so that the plasmon resonance band absorption cannot further occur in the original region. This leads to plasmon resonance bleaching, as a consequence saturation absorption occurs at near resonant excitation of plasmon band. Meanwhile, under the intense femtosecond laser beam excitation, the imbalanced distribution of thermalized and nonthermalized carriers can extend energy levels to induce a large modulation of absorption cross-section and can contribute to the nonlinear absorption, resulting in a thermal nature of the third-order nonlinearity of plasmonic media as previously demonstrated.[27,28] All these nonlinear optical processes involved will compete with each other to contribute to the complex nonlinear absorption and W-shaped open-aperture Z-scan traces near the plasmon resonance of $Cu_{2-x}Se$ nanocrystals. It is noted that the W-shaped Z-scan traces have also been observed for the hybrid semiconductor exciton/noble metal nanocrystals when the excitation wavelength is near the plasmon resonance band.[49,50]

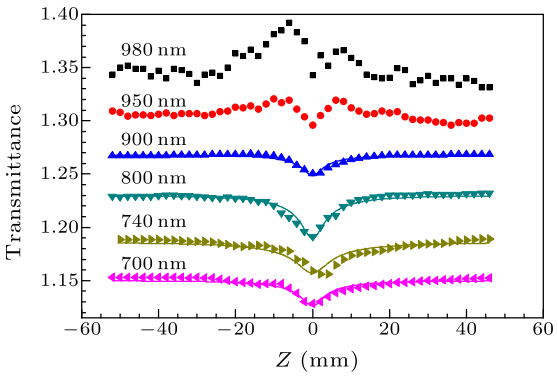

Fig. 3. Open-aperture Z-scan traces of $Cu_{2-x}Se$ nanocrystals at different excitation wavelengths.

As for the typical valley-shaped two-photon absorption feature at below-bandgap excitation in the range of 700–900 nm, the normalized Z-scan traces can be perfectly fitted with the simplified equation as follows:[45,48]

$$T_{\Delta\Psi(x)} = 1 - \frac{2(x^2+3)\Delta\Psi_0}{(x^2+9)(x^2+1)}, \quad (1)$$

where $x = z/z_0$ is the sample's coordinate according to the focal point of the lens, and $z_0 = \pi\omega_0^2/\lambda$ is the Rayleigh range of the beam with ω_0 and λ being the laser beam waist and wavelength of the excitation laser, respectively. The phase change contributed from the nonlinear absorption is $\Delta\Psi_0 = \beta I_0 L_{\text{eff}}/2$, where β denotes the third-order nonlinear absorption coefficient, I_0 refers to the irradiance intensity at focus, $L_{\text{eff}} = (1-e^{-\alpha_0 L})/\alpha_0$ is the effective sample thickness, with L being the sample'S thickness which is 1 mm, and $\alpha_0 = 0.35\,\text{mm}^{-1}$ at wavelength of 770 nm. The imaginary part of the third-order susceptibility $\text{Im}(\chi^{(3)})$ is related to β by the relation of $\text{Im}(\chi^{(3)}) = \lambda\varepsilon_0 n_0^2 c\beta/4\pi$, where n_0 is the linear refractive index, ε_0 and c are the permittivity of free space and velocity of light in vacuum, respectively.[43] The extracted values of $\text{Im}(\chi^{(3)})$ in the wavelength range of 700–900 nm are of the order of $1.9\text{–}2.7 \times 10^{-18}$ esu, as exhibited in Fig. 4. Thus the nonlinear optical absorption coefficient values are evaluated to be of the order of $4.30\text{–}7.38 \times 10^{-9}$ m/W.

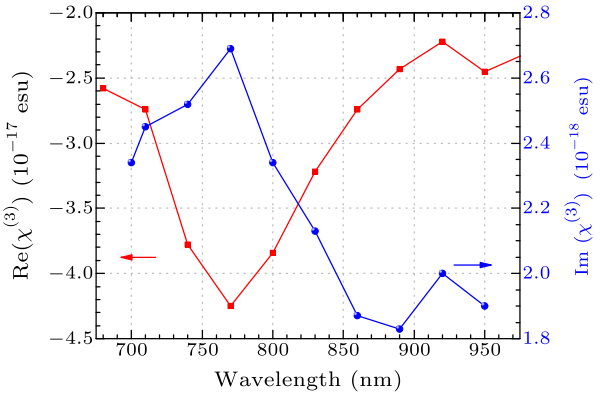

Fig. 4. Excitation wavelength dependence of the real (red line) and imaginary (blue line) parts of the third-order susceptibility $\chi^{(3)}$ of $Cu_{2-x}Se$ nanocrystals measured using the Z-scan technique.

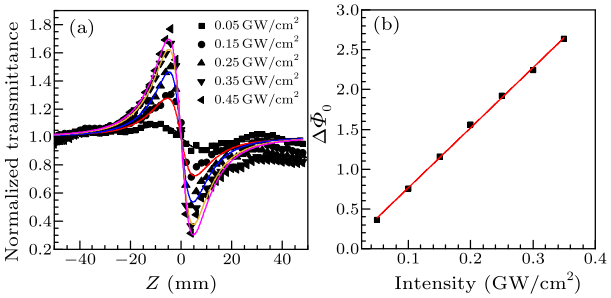

Fig. 5. (a) Closed-aperture Z-scan traces of $Cu_{2-x}Se$ nanocrystals excited at 770 nm with different incident intensities. The solid lines are the best-fitting curves. (b) Phase changes at different incident intensities extracted based on the measured data presented in (a).

The typical closed-aperture Z-scan traces taken at different laser excitation intensities with the excitation wavelength of 770 nm are shown in Fig. 5(a), so that the phase distortion induced purely by laser intensity-dependent refractive index can be deduced. At low irradiance intensity excitation, the peak-to-valley shape indicates that $Cu_{2-x}Se$ nanocrystals possess a negative value of the nonlinear refractive index. The closed-aperture Z-scan traces can be well fitted by[45,48]

$$T_{\Delta\Phi(x)} = 1 + \frac{4x\Delta\Phi_0}{(x^2+9)(x^2+1)}, \quad (2)$$

where $T_{\Delta\Phi(x)}$ is the normalized transmittance con-

tributed from the nonlinear phase distortion, and the phase change contributed from the nonlinear refraction is $\Delta\Phi_0 = k\gamma I_0 L_{\rm eff}$ with γ being the nonlinear index, and $k = 2\pi/\lambda$ being the wave vector. Nonlinear phase changes $\Delta\Phi_0$ under different intensities are evaluated based on results presented in Fig. 5(a) and displayed in Fig. 5(b) at low excitation intensity levels ($I_0 < 0.5\,{\rm GW/cm^2}$). A clear straight line for the plot of $\Delta\Phi_0$ versus I_0 indicates that there are no other higher-order nonlinear processes involved, and the nonlinear refraction is dominated by the bound-electronic transition induced ordinary third-order nonlinear effect at low excitation intensity.[39,49,50] The Kerr refractive index γ can then be deduced to be $2.64\times10^{-15}\,{\rm m^2/W}$ from the slope of this curve at low excitation intensities based on $\gamma = \Delta\Phi_0/kI_0L_{\rm eff}$. Therefore, the real part of the third-order nonlinear susceptibility ${\rm Re}(\chi^{(3)})$ is calculated to be $\sim4.45\times10^{-17}$ esu, based on the relation of ${\rm Re}(\chi^{(3)})({\rm esu}) = 2n_0^2\varepsilon_0 c\gamma$.[43] A series of closed-aperture Z-scan traces at different wavelengths and low irradiance intensity excitation are also performed, with the extracted third-order nonlinear susceptibility ${\rm Re}(\chi^{(3)})$ at different wavelengths shown in Fig. 4.

However, when the excitation intensity increases above $0.6\,{\rm GW/cm^2}$, the Z-scan traces at below-bandgap excitation of 770 nm starts to deviate from the symmetric peak-to-valley shape as shown in Fig. 6, with a peak-enhanced and valley-suppressed shape of Z-scan trace gradually showing up, implying the contribution from higher-order nonlinearity involving free-carrier excitation process. These asymmetrical Z-scan traces are typical combinations of the third- and fifth-order nonlinear responses, which can vary with excitation intensity and wavelength as usually observed in noble nanocrystals.[53,54] Here the bound-electronic nonlinearity has a third-order dependence on the incident irradiance, whereas the free-carrier nonlinearity has fifth-order dependence at high irradiance levels.[39]

It is known that the enhanced free-carrier process can strengthen the quantum confinement effect in plasmonic nanocrystals,[28] and further make considerable contribution to the nonlinear refractive response of self-doped $Cu_{2-x}Se$ nanocrystals, in which the free carriers are the holes in the valence band generated by copper vacancies.[22–29] Under the intense femtosecond laser excitation, the imbalanced distribution of thermalized and nonthermalized carriers can strongly modulate the energy distribution of hot carriers and absorption cross-section up to 10 times larger than that obtained in Au nanocrystals under the same optical fluence,[27,28] leading to the magnification of optical nonlinearity and higher-order nonlinear absorption response, though the density of free carrier in self-doped $Cu_{2-x}Se$ nanocrystals is relatively lower compared with the nobal metal nanocrystals. Thus the enhanced nonlinear optical coefficients of $Cu_{2-x}Se$ nanocrystals compared with other selenides such as ZnSe and CdSe[37,38] as listed in Table 1 are mainly associated with their unique properties whose optical nonlinearity is enhanced by the high-density free carriers at plasmon band excitation. The enhanced optical nonlinearity of $Cu_{2-x}Se$ nanocrystals over other selenides, in addition to the great capability to tune the plasmonic resonance by controlling the free-carrier density, makes the $Cu_{2-x}Se$ nanocrystals promising materials for the application of ultra-fast all-optical switching devices as well as nonlinear nanosensors.

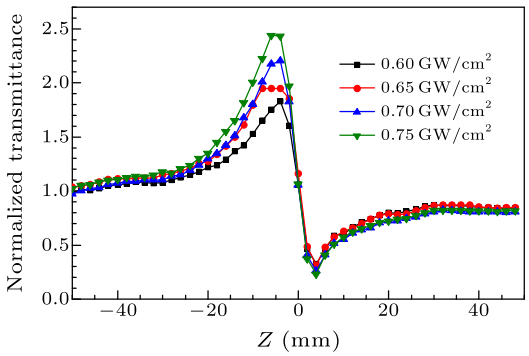

Fig. 6. Closed-aperture Z-scan traces excited at higher incident intensities at 770 nm.

Table 1. Nonlinear refractive index of different materials.

Material	Wavelength (nm)	Duration	Nonlinear refractive index ($\rm cm^2/W$)	Reference
CdSe quantum dot	520	225 fs	$(5.0\pm1.5)\times10^{-13}$	Ref. [37]
CdSe quantum dot	620	225 fs	$(8.2\pm2.4)\times10^{-14}$	Ref. [37]
CdSe/ZnS core shell quantum dots	580	225 fs	$(4.1\pm1.2)\times10^{-13}$	Ref. [37]
CdSe/ZnS core shell quantum dots	620	225 fs	$(2.5\pm0.7)\times10^{-13}$	Ref. [37]
ZnSe quantum dots	532	10 ns	2.46×10^{-13}	Ref. [38]
$Cu_{2-x}Se$ nanocrystals	770	150 fs	2.64×10^{-11}	present work

In conclusion, the Z-scan measurements have been performed for $Cu_{2-x}Se$ nanocrystals. Under below-bandgap excitation, the third-order nonlinear response of $Cu_{2-x}Se$ nanocrystals is observed to be greatly enhanced compared with the other selenides owing to the two-photon absorption contribution. However, a mixed feature of the reversed saturated absorption and saturated absorption exhibiting W-shaped Z-scan trace is observed when the excitation photon energy is tuned to be near the plasmon resonance band of $Cu_{2-x}Se$ nanocrystals, which is attributed to the state-filling of free carriers due to self-doping effect in $Cu_{2-x}Se$ nanocrystals as well as the hot carrier thermal effect upon intense femtosecond laser excitation. The enhanced nonlinear optical response and unique plasmonic band suggest that $Cu_{2-x}Se$ nano-

crystals are attractive for the promising application in the novel nonlinear optical devices.

References

[1] Alivisatos A P 1996 *Science* **271** 933
[2] Alivisatos A P 1996 *J. Phys. Chem.* **100** 13226
[3] Cao J C 2003 *Phys. Rev. Lett.* **91** 237401
[4] Cotter D, Burt M G and Manning R J 1992 *Phys. Rev. Lett.* **68** 1200
[5] Jia W, Douglas E P, Guo F and Sun W 2004 *Appl. Phys. Lett.* **85** 6326
[6] Anand B, Molli M, Aditha S, Rattan T M, Sai S S S and Kamisetti V 2013 *Opt. Commun.* **304** 75
[7] Yang W X, Chen A X, Huang Z and Lee R K 2015 *Opt. Express* **23** 13032
[8] Tripathi L N, Praveena M and Basu J K 2013 *Plasmonics* **8** 657
[9] Zhou X, Wenger J, Viscomi F, Cunff L L and Beal J 2015 *Nano Lett.* **15** 7458
[10] Potrick K and Huisken F 2015 *Phys. Rev.* B **91** 125306
[11] Kulakovich O, Strekal N, Yaroshevich, Maskevich S and Gaponenko S 2002 *Nano Lett.* **2** 1449
[12] Achermann M J 2010 *J. Phys. Chem. Lett.* **1** 2837
[13] Pelayo G D A F, Lasanta T, Bernechea M and Konstantatos G 2015 *Small* **11** 2636
[14] Song M, Wu B, Chen G, Liu Y, Ci X, Wu E and Zeng H 2014 *J. Phys. Chem.* C **118** 8514
[15] Yang W X 2015 *Opt. Lett.* **40** 4903
[16] Terzis A F, Kosionis S G, Boviatsis J and Paspalakis E 2016 *J. Mod. Opt.* **63** 451
[17] Schindel D and Singh M R 2015 *J. Phys.: Condens. Matter* **27** 345301
[18] Sadeghi S M, Wing W J and Gutha R R 2015 *Phys. Rev.* A **92** 023808
[19] Paspalakis E, Evangelou S, Kosionis S G and Terzis A F 2014 *J. Appl. Phys.* **115** 083106
[20] Carreño F, Antón M A, Melle S, Calderón O G and Cabrera-Granado E 2014 *J. Appl. Phys.* **115** 064304
[21] Li J B, Kim N C, Cheng M T, Zhou L and Hao Z H 2012 *Opt. Express* **20** 1856
[22] Gorbachev V V and Putilin I M 1973 *Phys. Status Solidi* A **16** 553
[23] Choi J, Kang N, Yang H Y, Kim H J and Son S U 2010 *Chem. Mater.* **22** 3586
[24] Zhu J B, Li Q Y, Bai L F, Sun Y F, Zhou M and Xie Y 2012 *Chem. Eur. J.* **18** 13213
[25] Klimov V I and Karavanskii V A 1996 *Phys. Rev.* B **54** 8087
[26] Kumar P and Singh K 2011 *Struct. Chem.* **22** 103
[27] Scotognella F, Valle G D, Kandada A R S and Dorfs D 2011 *Nano Lett.* **11** 4711
[28] Scotognella F, Valle G D, Kandada A R S, Zavelani-Rossi M and Longhi S 2013 *Eur. Phys. J.* B **86** 1
[29] Valle G D, Scotognella F, Kandada A R S, Zavelani-Rossi M and Li H 2013 *J. Phys. Chem. Lett.* **4** 3337
[30] Dorfs D, Haertling T, Miszta K, Bigall N C and Kim M R 2011 *J. Am. Chem. Soc.* **133** 11175
[31] Zhao Y X, Pan H C, Lou Y B, Qiu X F, Zhu J J and Burda C 2009 *J. Am. Chem. Soc.* **131** 4253
[32] Bussian D A, Crooker S A, Yin M, Brynda M and Efros A L 2009 *Nat. Mater.* **8** 35
[33] Guri V S, Prokopenko V B, Alexeenko A A, Wang S and Prokoshin P V 2001 *Mater. Sci. Eng.* C **15** 93
[34] Yumashev K V, Gurin V S, Prokoshin P V, Prokopenko V B and Alexeenko A A 2001 *Phys. Status Solidi* B **224** 815
[35] Gurin V S, Prokopenko V B, Alexeenko A A, Wang S X, Yumashev K V and Prokoshin P V 2001 *Int. J. Inorg. Mater.* **3** 493
[36] Gurin V S, Alexeenko A A, Zolotovskaya S A and Yumashev K V 2006 *Mater. Sci. Eng.* C **26** 952
[37] Gerdova I and Hache A 2005 *Opt. Commun.* **246** 205
[38] Jiao Y, Yu D B, Wang Z R and Sun X Q 2007 *Mater. Lett.* **61** 1541
[39] Said A A, Sheik-Bahae M, Hagan D J, Wei T H and Wang J 1992 *J. Opt. Soc. Am.* B **9** 405
[40] Jia G Z, Lou W K, Cheng F, Wang X L and Yao J H 2015 *Nano Res.* **8** 1443
[41] Jia G Z, Wang P, Wu Z G, Li Q and Zhang Y B 2015 *AIP Adv.* **5** 087176
[42] Kriegel I, Jiang C Y, Rodríguez-Fernandez J, Schaller R D and Talapin D V 2012 *J. Am. Chem. Soc.* **134** 1583
[43] Statkutė G, Mikulskas I, Tomašiūnas R and Jagminas A 2009 *J. Appl. Phys.* **105** 113519
[44] Luther J M, Jain P K, Ewers T and Alivisatos A P 2011 *Nat. Mater.* **10** 361
[45] Sheik-Bahae M, Said A A, Wei T H, Hagan D J and van Stryland E W 1990 *IEEE J. Quantum Electron.* **26** 760
[46] Sheik-Bahae M, Hagan D J and van Stryland E W 1990 *Phys. Rev. Lett.* **65** 96
[47] Hutchings D C and van Stryland E W 1992 *J. Opt. Soc. Am.* B **9** 2065
[48] Sheik-bahae M, Said A A and van Stryland E W 1989 *Opt. Lett.* **14** 955
[49] Unnikrishnan K P, Nampoori V P N, Ramakrishnan V, Umadevi M and Vallabhan C P G 2003 *J. Phys.* D **36** 1242
[50] Nan F, Zhang Y F, Li X G, Zhang X T, Li H and Zhang X H 2015 *Nano Lett.* **15** 2705
[51] Sheik-Bahae M, Hutchings D C, Hagan D J and van Stryland E W 1991 *IEEE J. Quantum Electron.* **27** 1296
[52] Cotter D, Burt M G and Manning R 1992 *Phys. Rev. Lett.* **68** 1200
[53] Yu B H, Zhang D L, Li Y B and Tang Q B 2013 *Chin. Phys.* B **22** 014212
[54] Fan G H, Qu S L, Guo Z Y and Li Z G 2012 *Chin. Phys.* B **21** 047804